

The role of irradiation on deformation-induced martensitic phase transformations in face-centered cubic alloys

Janelle P. Wharry^{1,a)} Keyou S. Mao²

AUI ¹Purdue University, West Lafayette, Indiana 47905, USA

²Oak Ridge National Laboratory, Oak Ridge, Tennessee 37830, USA

a) Address all correspondence to this author. e-mail: jwharry@purdue.edu This paper has been selected as an Invited Feature Paper.

Received: 18 December 2019; accepted: 20 March 2020

Localized deformation, including that by the deformation-induced shearing martensitic phase transformation, is responsible for hardening and embrittlement in irradiated face-centered cubic alloys. These localized deformation processes can have profound consequences on the mechanical integrity of common structural metals used in extreme radiation environments such as nuclear reactors. This article aims to review and understand exactly how irradiation affects the martensitic phase transformation in face-centered cubic alloys, with an emphasis on austenitic stainless steel, given its ubiquity in the archival literature. The influence of irradiation on stacking fault energy and subsequent implications on the phase transformation are discussed. Mechanisms by which irradiation-induced microstructures enhance the phase transformation are also described, including the surface energy contribution of irradiation-induced cavities (i.e., voids and bubbles) toward the critical martensite nucleation energy, and partial dislocation—cavity interactions. A deformation mechanism map illustrates how irradiation-induced cavities can modulate the martensitic transformation pathway.

Introduction

Irradiation of metals and alloys with energetic particles causes severe degradation of mechanical performance, most notably through hardening and embrittlement. These phenomena dramatically compromise the safety, operating margins, and lifetime of structural and cladding components of nuclear fission and fusion reactors. Mechanistically, the most significant contributor to irradiation hardening and embrittlement in face-centered cubic (fcc) metals and alloys tested at low temperatures (i.e., ≤400 °C, outside of the creep regime) is the tendency toward localized deformation [1, 2, 3].

Localized deformation in fcc metals and alloys can occur through several modes, including dislocation channeling [4, 5], slip [6], twinning [7], and the so-called martensitic phase transformation [8, 9]. The martensitic transformation is a diffusionless phase transformation, wherein fcc γ Fe austenite reverts to hexagonal close-packed (hcp) ϵ martensite or bodycentered cubic (bcc) α' martensite. All of the aforementioned localized deformation mechanisms are known to interact in a complex manner [10]. In nonirradiated materials, these mechanisms and their interactions are dependent upon

deformation temperature, strain, strain rate, and stacking fault energy (SFE). Meric de Bellefon and van Duysen [10] have recently reviewed these low-temperature deformation mechanisms in austenitic stainless steels (SSs).

Under irradiation, localized deformation modes can occur more readily. Specifically, the activation of dislocation channels, deformation twins, and deformation-induced martensites occurs at higher deformation temperatures, lower strains, and/ or lower strain rates than in nonirradiated materials [1, 11, 12]. Most studies on deformation of irradiated fcc alloys have focused on dislocation channeling or deformation twinning, rather than on the martensitic transformation. As such, the mechanisms underpinning the irradiation enhancement of martensitic transformations remain only moderately understood. Historically, most studies have tended to ascribe deformation-induced martensites to the twinning associated with irradiation-induced dislocation loops (i.e., interstitial-type defects) [13, 14, 15, 16]. Recently, however, porosity has been shown to enhance the martensitic transformation in shape memory alloys [17, 18, 19] through surface energy effects. A series of systematic deformation studies on neutron-irradiated

© Materials Research Society 2020 cambridge.org/JMR



3

4

5

8

10

11

12

13

14

15

16

17

18

19

20

21

22

23

24

25

26

27

28

29

30

31

32

33 34

35

36

37

38

39 40

41

42

43

44

45

46 47

48

49

50

51

52 53

54

55

56

57

58

59 60 AISI 304L SS have also corroborated the central role of cavities (i.e., irradiation-induced voids and/or bubbles, rather than metal casting–induced pore defects) in the activation of martensitic transformations. Thus, there is considerable evidence throughout the archival literature on the importance of both interstitial-type (e.g., loops) and vacancy-type (e.g., cavities) irradiation defects on the martensitic phase transformation.

This article will review the effects of irradiation on localized deformation, with specific focus on the deformation-induced martensitic phase transformation. This article will begin with a brief overview of the well-understood mechanisms by which irradiation enhances dislocation channeling and deformation twinning. Subsequently, the article will review the existing literature on the deformation-induced martensitic phase transformation in irradiated materials. The role of SFE, interstitial type, and vacancy-type irradiation-induced defects on the deformation-induced martensitic phase transformation pathway will be surveyed. Finally, a deformation mechanism map will be generated based on observations in the archival literature, revealing the role of irradiation-induced cavities on the martensitic phase transformation pathway.

Overview of localized deformation in irradiated fcc alloys

The interplay of low-temperature deformation mechanisms can be understood by considering the deformation mechanism maps from the fcc γ austenite phase in high-Mn steels commonly known as transformation-induced plasticity (TRIP) or twinning-induced plasticity (TWIP) steels, Fig. 1(a). The influence of SFE, strain, and test temperature on deformation mode is similar in 300-series austenitic SSs as in TRIP/TWIP steels. In general, with decreasing SFE and/or test temperature, the deformation mechanism tends to evolve from dislocation glide to twinning to deformation-induced martensitic transformations [20, 21]. This evolution in deformation mode corresponds to a general increase in ultimate tensile stress (UTS) as well as a peak in uniform elongation (UE) when deformation twinning is predominant [Fig. 1(a)]. The α' martensites tend to be lower SFE, lower temperature phases than ε martensites, although complex deformation microstructures exhibiting a combination of α' martensites, ϵ martensites, and/or twins can be observed under varying loading conditions, strains, and alloy compositions [12, 20, 21, 22, 23, 24, 25, 26, 27, 28].

Irradiation produces a supersaturation of point defects—vacancies and interstitials—in metals and alloys; over time, these defects alter the microstructure and can subsequently have profound impacts on deformation mechanisms [29]. Irradiation-induced Frenkel pair defects can recombine, remain as freely migrating vacancies and interstitials, diffuse to point

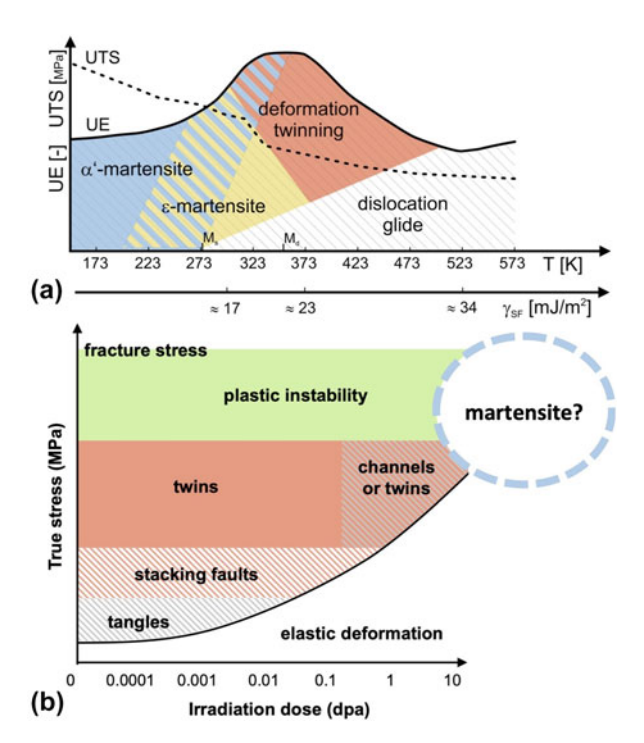


Figure 1: Deformation mechanism maps for (a) TRIP/TWIP steels as a function of temperature and SFE, from Ref. 20 and (b) irradiated austenitic SS as a function of irradiation dose, adapted from Ref. 34. (color online)

defect sinks (e.g., grain boundaries), or diffuse into clusters of vacancies or clusters of interstitials [30]. With increasing irradiation fluence (i.e., dose), a defect microstructure evolves, the most notable features of which are dislocation loops and voids. Dislocation loops are two-dimensional defects typically formed by collapse of interstitial-type or vacancy-type plateletlike clusters. However, in austenitic SS irradiated at nuclear reactor-relevant conditions, there is a strong bias for the formation of interstitial-type Frank loops [29, 31, 32, 33]. Voids are three-dimensional vacancy-type defects, typically faceted along crystallographic planes [29, 32, 33]. In-reactor irradiation also produces transmutation gases, often He in austenitic SS, which can agglomerate into bubbles [30]. Bubbles can be difficult to distinguish from voids, although their internal gas pressure creates a spherical, nonfaceted appearance [30].

Under irradiation, Byun et al. [34] suggest that a similar evolution in deformation mechanism occurs in austenitic SS as in TRIP/TWIP steels, although the irradiation fluence—rather than SFE—is believed to strongly influence the operative deformation mechanism. The influence of irradiation on deformation mechanisms is mapped for irradiated austenitic SS, as shown in Fig. 1(b). With increasing load, the deformation mechanism evolves from dislocation-mediated to formation of stacking faults to deformation twinning [34]. We also add a theorized region of martensitic transformation at higher irradiation doses, based on reports in the archival literature to



3

8

10

11

12

13

14

15

16

17

18

19

2.0

21

22

23

24

25

26

27

28

29

30

31

32

33 34

35

36

37

38

39

40

41

42

43

44

45

46 47

48

49

50

51

52 53

54

55

56

57

58

59 60 be presented later in this review [blue dashed region, Fig. 1(b)]. Irradiation-induced embrittlement occurs at high doses by eliminating dislocation-mediated plasticity in favor of plasticity through localized channeling or deformation twinning.

Historically, studies on localized deformation of irradiated materials have most commonly focused on dislocation channeling [3, 35, 36, 37], primarily in austenitic SSs, and often in the context of stress corrosion cracking (SCC) susceptibility [5, 38]. Dislocation channeling in irradiated materials occurs when gliding dislocations are pinned by clusters of irradiationinduced defects, absorb these defects to become unpinned, and then cross-slip under increasing stress [39]. Multiple passing dislocations ultimately create a defect-free path, or "channel," characterized by dense dislocation tangles along the channel-matrix wall [40]. Subsequent dislocations can then easily glide in channels in a highly localized deformation process [39, 40]. There is evidence that channel formation occurs most readily at grain boundary triple junctions [5] and in the middle of grain boundaries between grains having high Schmid factor mismatch [41]. Mechanisms of dislocation channeling in irradiated materials, and the interaction between dislocation slip, cross-slip, and channeling, have recently been reviewed in Refs. 42 and 43.

The idea that irradiation enhances the propensity for deformation twinning has also been established in the literature for decades. The seminal Cottrell & Bilby [13] deformation twinning mechanism suggests that prismatic loops can serve as sources of twinning partials. A decade later, Venables [14, 15] confirmed that neutron irradiation-induced prismatic loops cause gliding dislocations to dissociate into partial dislocations, which then jog to create a twin source, as sources of twinning partials. In the 1990s through 2000s, a series of studies from Byun, Hashimoto, Lee, and colleagues [2, 4, 7, 11, 12, 16, 34, 44, 45, 46, 47, 48, 49, 50] have shown that a wide variety of neutron irradiations of 300 series austenitic SSs conducted over temperatures ranging ~200-450 °C and doses ranging ~0.1-40 displacements per atom (dpa), and tensile tested over a wide range of temperatures ranging −150 to 400 °C, causes the room temperature deformation mechanism to change from dislocation-mediated to deformation twinning. Irradiation-induced Frank loops and other planar defects act as deformation twin nucleation sites [16]. Additionally, Gussev et al. [41] have found that dislocation channels exhibit a twinning nature in neutron irradiated AISI 304 SS and a model 304 SS, emphasizing the complex interplay between these low-temperature deformation mechanisms.

Meanwhile, the influence of irradiation on deformationinduced phase transformations has received significantly less attention and remains poorly understood [1, 2, 3]. The deformation-induced martensitic transformation is believed to occur through three possible pathways [26, 46, 51, 52, 53, 54, 55]:

- (i) strain-induced: γ austenite transforms to a twin structure, and then to α' martensite, $\gamma \to T \to \alpha'$;
- (ii) stress-induced: direct $\gamma \rightarrow \alpha'$; or
- (iii) stress-induced: via metastable hcp ϵ martensite, $\gamma \to \epsilon \to \alpha'.$

Although a few studies have observed the deformation-induced martensitic transformation in neutron [8, 11, 16, 18, 46, 48, 56, 57, 58, 59, 60] or ion [61, 62] irradiated SSs, they have also observed complex deformation microstructures containing various combinations of α' martensites, ϵ martensites, deformation twins, and/or stacking faults. Hence, it remains unclear which martensitic transformation pathway(s) are active, and, specifically, how irradiation-induced defects enable the martensitic transformation. The remainder of this review will focus on three primary mechanisms through which irradiation influences the propensity for the deformation-induced martensitic transformation: (a) SFE, (b) cavity surface energy, and (c) vacancy-type and interstitial-type defect morphologies.

Irradiation influences on deformationinduced martensitic transformation

Effect of irradiation on stacking fault energy

The SFE (γ_{SFE}) is well known to influence the mechanical properties and deformation mechanisms of metallic alloys [63]. That is, under identical loading conditions, low SFE alloys are inclined to form twins and martensite, whereas higher SFE alloys tend to undergo dislocation slip [46, 64]. Hence, it is worth considering first the role of irradiation on SFE. Several studies have suggested that irradiation reduces the bulk SFE in a material. Specifically, Hashimoto and Byun [11] irradiated an AISI 316 SS to 0.1 dpa over 65–100 °C. They observe the $\gamma \rightarrow$ α' transformation over a range of strain levels at room temperature and suggest that the transformation is induced by spreading a Shockley partial over successive (111) fcc planes, which effectively reduces SFE. Models have also shown dislocation channel widths exhibit a power law dependence on irradiation-induced defect cluster size, number density, and distance from dislocation source [65], suggesting that SFE is reduced with larger and more populous irradiation defects.

It is well established SFE is highly composition dependent. In order to control SFE—and hence, the deformation mechanism—alloy designers often employ the approach of modifying the global chemical composition. Nearly a half-century ago, Latanision and Ruff [66] showed that cyclic heating of austenitic Fe-Cr-Ni alloys induces an irreversible change in intrinsic SFE due to substitutional solute atmospheres around dislocations. Since then, generalized SFE-composition relationships have been identified for Fe-base alloys; Mn [21] and C



3

4

8

10

11

12

13 14

15

16

17

18

19

2.0

21

22

23

24

25

26 27

28

29

30

31

32

33 34

35

36

37

38

39

40

41

42

43

44

45

46 47

48

49

50

51

52 53

54

55

56

57

58

59 60 [67] increase SFE, whereas N decreases SFE [68, 69], although these trends may differ for different host alloys [70]. Even our understanding of the temperature dependence of SFE is tied to composition effects, specifically solute segregation and diffusion with increasing temperature [71].

The work in the archival literature has largely focused on the influence of composition on SFE, with almost no understanding of the effect of microstructure-not to mention, the irradiated microstructure—on SFE. To our knowledge, only a few studies [72, 73] have expressly focused on understanding the role of point defects or microstructure on SFE. Jun and Choi [73] focus on grain size and show an inverse relationship between grain size and SFE. An increase in SFE has also been associated with severe plastic deformation (SPD) such as highspeed drawing [74], although it is uncertain whether this SFE increase is associated with the introduction of dislocations during the SPD process, grain size refinement, and/or chemical inhomogeneities. Asadi et al. [72] conduct density functional theory (DFT) calculations to show that the generalized SFEs in fcc Ni, Cu, and Al decrease significantly when a single atomic vacancy is situated on the stacking fault plane. In fact, the stable and unstable SFEs progressively decrease by up to ~10% when vacancy fraction is increased up to \sim 12.5% [Fig. 2(a)]. But more critically, Asadi et al. [72] show that single and divacancies on the stacking fault plane induce highly localized spatial variations in SFE as a function of displacement along a crystallographic direction [Fig. 2(b)].

The concept of spatially varying local SFEs is especially applicable for irradiated metals and alloys because of the ~nanometer length scale between defects that strongly influences mechanical behavior [75] as well as the propensity for grain-boundary radiation-induced segregation (RIS) [76]. To some extent, localization of SFE variations has also been explored through first-principle calculations in concentrated solid-solution alloys [77]. They propose a model to predict SFE based on localized bond breaking/forming, and suggest that local atomic configurations and electronic structure primarily influence SFE. Electronic structure is well known to affect SFE and phase stability: Hume-Rothery and coworkers' seminal 1957 study [78] establishes that the fcc structure is stable when d-electrons make only a small contribution to bonding, that is, high SFE per Ref. 79. As the *d*-electron contribution to bonding increases, phase stability favors first the hcp and then the bcc structure [78].

Hickel et al. [67] demonstrate the implications of extremely localized spatial variations (~few nm) in SFE. Although their SFE variations are composition-based, rather than being associated with defects, they nevertheless show that stacking faults in Fe–Mn–C steels will form exclusively in the lowest SFE regions. Hence, it is plausible that a population of irradiation-induced defects can similarly introduce localized spatial

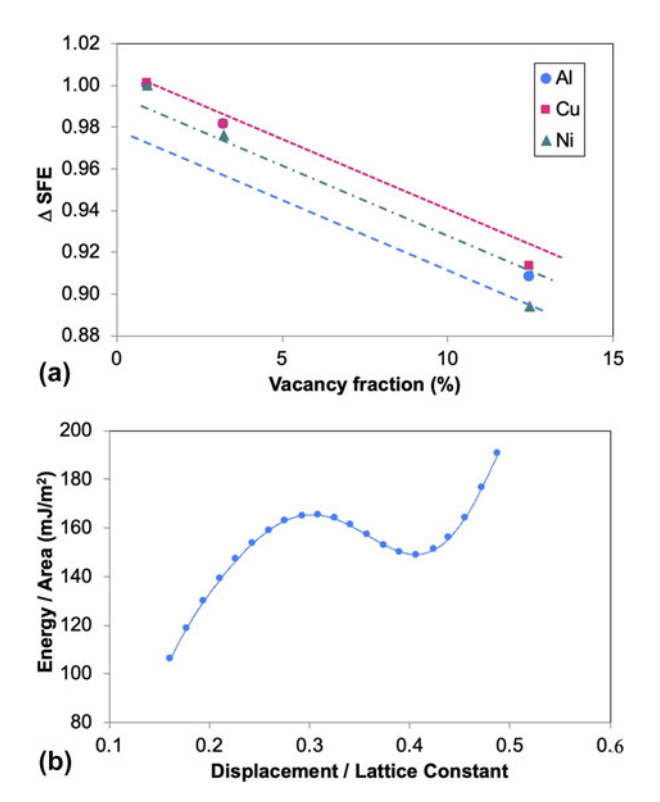


Figure 2: Change in SFE varies as a function of (a) vacancy fraction in the material, and (b) spatial position from di-vacancy, normalized to lattice constant; figures adapted from Ref. 72. (color online)

variations or fluctuations in SFE. In turn, these SFE variations could subsequently enable the nucleation, growth/propagation, and termination of martensite needles at various positions around the irradiation-induced defect of interest.

To our knowledge, there have not been any direct studies that have either measured or calculated the change in SFE with irradiation. However, some experimental evidence of the deformation implications of SFE variations associated with irradiation-induced defects can be extrapolated from the work of Mao et al. [80], who conducted nanoindentation on AISI 304L SS hexagonal reflector blocks irradiated in EBR-II to \sim 23 dpa at 415 °C. The irradiated microstructure contained 19.3 \pm 7.6 nm voids at a number density of $1.33 \pm 0.33 \times 10^{21} \text{ m}^{-3}$, having facets on {111} planes, as well as network dislocations and dislocation lines at such a high number density that they are indistinguishable from one another. Following nanoindentation, characterization of the plastic zone beneath the indent revealed that the $\gamma \rightarrow \alpha'$ transformation occurred. Mao and coworkers [80] further investigated the deformation microstructure, specifically the α' martensite needle tips. They found that the tips are either coincident with voids (Fig. 3) or terminate in the γ austenite matrix without a resolvable association with any irradiation-induced defects. Given that proximity to vacancies can effectively lower the SFE [72], it is theorized that the voids can serve as sites of martensite



2

3

4

10

11

12

13 14

15

16

17

18

19

2.0

21

22

23

24

25

26 27

28

29

30

31

32

33 34

35

36

37

38

39

40

41

42

43

44

45

46

47

48

49

50

51

52

53

54

55

56

57

58

59

60

nucleation, and that the martensite needles terminate in the higher SFE matrix, that is, further away from irradiation-induced vacancies.

Role of irradiation-induced cavities and surface energy

Because irradiation-enhanced twinning is known to occur through irradiation-induced Frank and prismatic loops [13, 14, 15, 16], the influence of these loops and other planar defects has also been considered for the irradiation-enhanced deformation-induced martensitic transformation. But there is considerable debate surrounding the nucleation of deformation-induced martensite in irradiated alloys, wherein inconsistent experimental results have ascribed martensite nucleation to virtually every possible microstructural feature. Specifically, there is experimental evidence of deformation-induced martensites in irradiated austenitic SS nucleating on—or associated with—twins [60], stacking faults [16, 60], dislocation channels [8, 11, 16, 57, 65, 81], and/or grain boundaries [57, 82]. However, recent work on shape-memory alloys [17] has suggested that porosity may be an influential factor controlling the deformation-induced austenite-to-martensite phase transformation. These findings thus suggest that irradiation-induced cavities may play a critical role in governing the operative deformation mechanisms of irradiated metals and alloys. It has been argued that pores or cavities enable the martensitic transformation either through surface energy contributions, or by hindering partial dislocation motion through a hardening process [46, 47, 80, 83].

In Ni-Mn-Ga shape-memory alloys, a magnetic fieldinduced strain (MFIS) induces a reversible austenite to martensite phase transformation, which occurs through twin boundary motion [17]. The transformation is inhibited in fine-grained Ni-Mn-Ga because grain boundaries constrain the twin boundary motion [17]. However, Chmielus et al. [17] have recently shown that porosity-introduced through a metallic foam nanoarchitecturing process—enhances the capacity of Ni-Mn-Ga to accommodate MFIS by eliminating some of the constraints hindering twin boundary motion. Similarly, Han et al. [18] introduced porosity into a Ni_{53,5}Fe_{19,5}Ga₂₇ shape-memory alloy using He implantation. They found that a 5- to 10-nm dispersion of He nanobubbles promoted the nucleation of martensite embryos and aided in the reversible austenite-martensite phase transformation. Han et al. [18] explained the phenomenon by suggesting that the internal surface area of the He bubbles compensates the surface energy contribution to the total free energy of the martensitic phase transformation due to the large surface-area-to-volume ratio of the martensite in a microscale plastic region (e.g., created

through microcompression pillar testing and nanoindentation). Additionally, Levin et al. [19] use phase-field simulations to show the stress-induced martensitic phase transformation occurs at nanovoids.

Recent deformation studies on austenitic SS reported by Mao et al. [9, 83] corroborate that Chmielus' [17] and Han's [18] ideas from shape-memory alloys can be extended to other fcc alloy systems. Specifically, Mao [83] studies AISI 304L SS reflector blocks irradiated in EBR-II to 0.4 dpa at 415 °C, which contain <1 appm He. They observe 16.3 \pm 6.1 nm cavities (i.e., He bubbles and/or voids) at a number density of 1.01 \pm 0.78 \times 10^{20} m^{-3} , along with a 6.11 $\pm 0.31 \times 10^{13} \text{ m}^{-2}$ density of Frank loops [Figs. 4(a) and 4(b)]. Mao's irradiated specimen was subsequently laser welded, which had a partial annealing effect—cavities were reduced in size to 11.4 ± 3.9 nm and their number density decrease by an order of magnitude to 4.99 ± $2.38 \times 10^{19} \,\mathrm{m}^{-3}$ in the weld heat-affected zone (HAZ), but the dislocation microstructure largely remained unaltered at a number density of $4.73 \pm 1.13 \times 10^{13} \text{ m}^{-2}$ [Figs. 4(f) and 4(g)]. Micropillars were created on {101} grains in both the irradiated and HAZ specimens, and underwent in situ scanning electron microscopic (SEM) compression, Figs. 4(c), 4(d), 4(h), and 4(i). The HAZ deformed through incipient twinning, whereas the irradiated specimen deformed via the $\gamma \to \epsilon$ transformation, Figs. 4(e) and 4(j). The critical stress on the martensitic deformation plane exceeds the critical twinning stress by >400 MPa. These results suggest that although the irradiation-induced dislocation microstructure in the HAZ may initiate twinning, the deformation-induced martensitic transformation in the irradiated base metal is more likely associated with the presence of cavities. It should be noted, however, that changes in stress state [84] and local chemistry [85] typical of laser welding were not considered in the aforementioned changes in deformation mechanisms.

Cavities may promote the martensitic transformation by increasing the Orowan hardness of the material, requiring extreme stresses to move dislocations through or around cavities [86, 87]. These stresses may be sufficiently higher than the threshold stress for the martensitic transformation. Alternatively, surface energy could explain how cavities promote the transformation [9, 18]. The transformation is favored if ΔG + $U \ge \Delta G_{\rm C}$, where ΔG is the Gibbs free energy, U is the strain energy corresponding to the externally applied stress [51, 88], and the critical free energy of the martensitic transformation is $\Delta G_{\rm c} = 2100$ J/mol [51]. Internal surfaces of irradiation cavities can contribute to the total free energy change (ΔG) [18]. If the cavity number density is sufficiently high, then their contribution to ΔG can ensure that the inequality $(\Delta G + U \ge \Delta G_C)$ is met at lower temperatures and/or applied loads than in unirradiated materials.



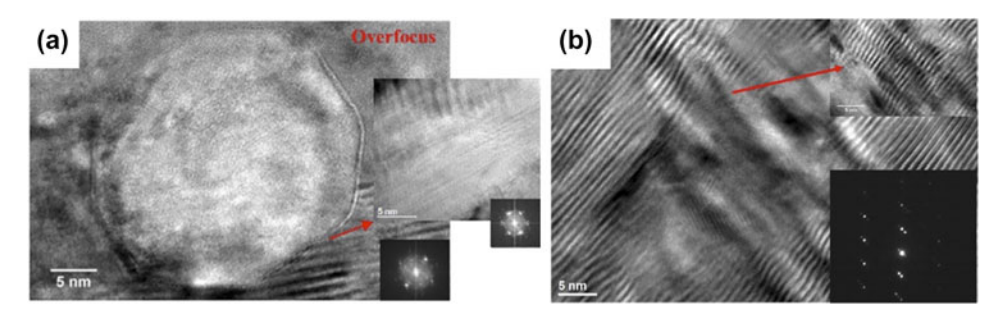


Figure 3: HRTEM micrographs of martensite tips (a) coincident with void surface, and (b) in matrix, from Ref. 80. (color online)

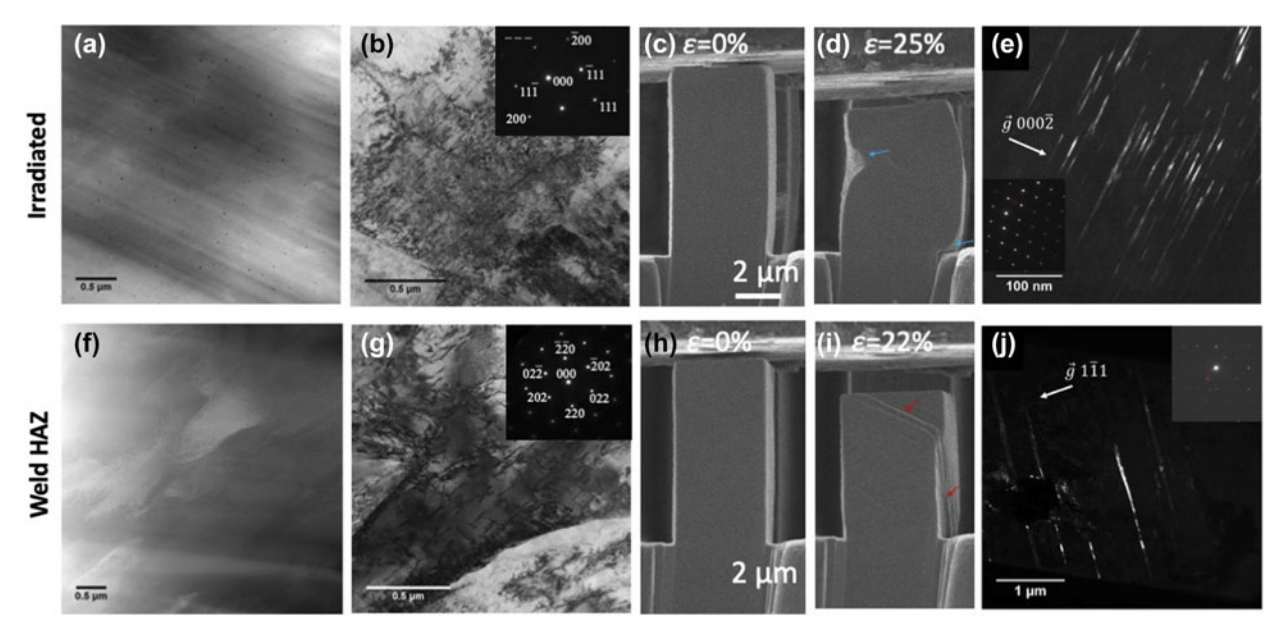


Figure 4: TEM micrographs of (a) voids and (b) dislocation loops, (c and d) still-frames from in situ SEM micropillar compression tests in [101] grains, and (e) deformation-induced ε martensite in irradiated 304 SS; (f) voids, (g) loops, (h and i) micropillar compression tests, and (j) deformation twins, in irradiated 304 SS weld HAZ, from Ref. 83. (color online)

Relative influences of irradiation-induced vacancyand interstitial-type defects

In this section, we consider the microstructural requirements for each stress-induced martensitic transform pathways, $\gamma \rightarrow$ α' and $\gamma\to\epsilon\to\alpha'.$ The $\gamma\to\epsilon\to\alpha'$ transform has been described by Bogers and Burgers [89] using their hard-sphere model, and further explained by Olson and Cohen [90] using a shearing-intersection model, Fig. 5. The Bogers-Burgers-Olson-Cohen (BBOC) model suggests that the $\gamma \to \epsilon$ transformation occurs initially, and the intersection of ε-martensite bands with stacking faults enables completion of the $\epsilon \to \alpha'$ transformation. Nucleation of metastable ϵ martensite involves dislocation motion: specifically, shear on γ austenite {111} planes produces an hcp-ε plate by slip or twinning [91]. To subsequently form α' martensite from ϵ martensite, the BBOC model requires the shear of partial dislocations at the intersection of the two preformed hcp-ε plates [90], Fig. 5. The implication, in the context of an irradiated microstructure, is that if irradiation-induced cavities are sufficiently small, Shockley partials can cut through them to form stacking faults [92]. Continual partial dislocation slip will progressively reduce cavity dimensions and increase their ellipticity [58], ultimately leading to twin nucleation [92] and the production of ϵ martensite plates. Additionally, an irradiated microstructure containing interstitial Frank and prismatic loops could also induce twinning to nucleate ϵ martensite plates [60].

On the other hand, the direct $\gamma \to \alpha'$ transformation requires an increase in cavity number density and size, which will interact with dislocations to form jogs, over which dislocations will climb [93]. If these cavities—and hence, jogs—exist at a sufficiently high number density, the extent of dislocation climb will inhibit twinning. Cavity size is also a governing factor, because partial dislocation interactions with larger voids can result in recombination into perfect dislocations [93], suppressing twinning. These processes ultimately inhibit dislocation glide into twinning shear, which eliminates

© Materials Research Society 2020 cambridge.org/JMR



2

3

10

11

12

13 14

15

16

17

18

19

20 21

22

23

24

25

26 27

28

29

30

31

32

33 34

35

36

37

38

39

40 41

42

43

44

45

46 47

48

49

50

51

52 53

54

55

56

57

58

59 60

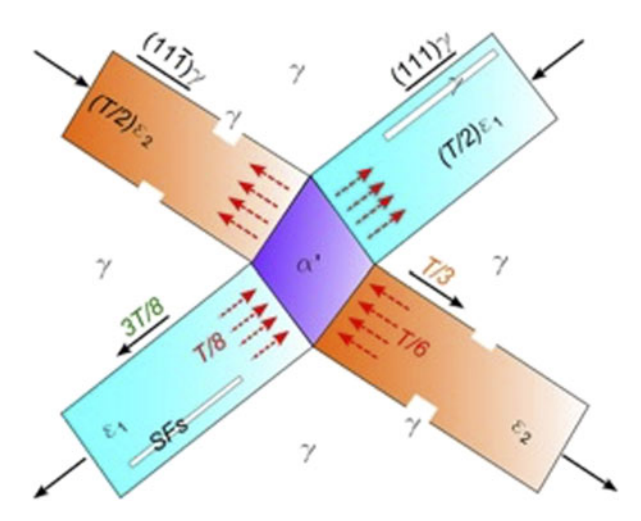


Figure 5: Cartoon illustration of BBOC shearing-intersection model, from Ref. 90. (color online)

the intermediary steps necessary to nucleate metastable ϵ martensite. A high number density of stress concentrations at large cavities ultimately result in the direct $\gamma \to \alpha'$ transformation [26]. This is corroborated by experimental observations from Gusev et al. [56], who irradiated low-Ni steels in the BN-350 fast reactor. Under tensile loading, they suggest that the α' martensitic transformation occurs most readily at \geq 20 dpa; one can imagine that at this dose range, irradiation-induced voids are large and populous.

In another study, Mao et al. [80] conducted nanoindentation on {110} grains in AISI 304L SS neutron irradiated at 415 °C to 23 dpa containing ∼3 appm He [9]. This specimen was also laser welded, much like the welding outlined in Section "Role of irradiation-induced cavities and surface energy." In this specimen, cavity sizes are relatively unchanged with welding, ranging 16.2-20.9 nm across the HAZ and base metal, but the cavity number density is reduced by two orders of magnitude in the HAZ at $1.4 \pm 1.3 \times 10^{19} \,\mathrm{m}^{-3}$ as compared with 1.2 \pm 0.3 \times 10²¹ m⁻³ in the base metal. TEM lamellae were prepared from the nanoindentation plastic zone to observe the deformation microstructure. The neutron irradiated specimen has a high density of α' martensite laths [Figs. 6(a) and 6(b)]. Meanwhile, the weld HAZ has undergone the $\gamma \to \varepsilon \to \alpha'$ transformation [Figs. 6(c) and 6(d)]. Brightfield TEM shows the formation of hcp-ε shear bands beneath the indent and indicates the two hcp-ε plates intersect to form α' martensite, consistent with the BBOC model. The two ϵ plates have two arrays of $a/6\langle 112\rangle$ partial dislocations on every second and every third $\{111\}_{\gamma}$ plane.

Differences in deformation mechanism in irradiated 304L SS are attributed to differences in pre-deformation microstructures. The irradiated specimen contained a high number density of large cavities (i.e., He bubbles and/or voids), as well as a high density of Frank loops [Fig. 6(a)]. The HAZ

microstructure was annealed compared with the irradiated specimens: cavity number density was dramatically reduced, but loops primarily remained present [Fig. 6(c)]. In irradiated austenitic SSs, faulted Frank loops form on {111} habit planes with Burgers vectors $\mathbf{b} = \mathbf{a}_0/3\langle 111 \rangle$ [94]. These are interstitialtype loops at irradiation temperatures >360 °C [94]. At irradiation temperatures ≤300 °C, Frank loops are small in diameter (i.e., <10 nm), making it difficult to discern their nature, but they are typically assumed to represent the interstitial-driven component of the irradiated microstructure [94]. Prismatic dislocation loops, with Burgers vectors $b = a_0$ / $2\langle 110\rangle$ on $\{111\}$ habit planes, can be of either interstitial or vacancy type, and form directly from irradiation damage cascade collapse or from Frank loop unfaulting [94]. Because interstitial diffusion and the formation of interstitial-type defects occur faster than vacancy diffusion [30], with increasing irradiation dose, vacancy-type defects become a more dominant contribution to the microstructure, and thus the transformation shifts from the metastable $\gamma \to \epsilon \to \alpha'$ pathway to the direct $\gamma \rightarrow \alpha'$ pathway.

The size and number density of vacancy-type defects, relative to the size and number density of interstitial-type defects, control whether an irradiated material will deform via the $\gamma \rightarrow \alpha'$ transformation or through the $\gamma \rightarrow \epsilon \rightarrow \alpha'$ mechanism [93]. The irradiation dose evolution of defects must be considered for their influence on deformation mechanisms. Chmielus et al. [17] also acknowledge the importance of porosity size, noting that pore sizes smaller than grains can more effectively accommodate the phase transformation. Likewise, considering all three of Mao and coworkers' published studies [9, 80, 83] on deformation in neutron irradiated 304L SS, one can extract a deformation mechanism map based on cavity morphology and He concentration (Fig. 7). This map reveals that the direct $\gamma \rightarrow \alpha'$ transformation can occur when vacancy-type defects dominate the irradiated microstructure, whereas the $\gamma \, \to \, \epsilon \, \to \, \alpha'$ transformation (or the $\gamma \, \to \, \epsilon$ transformation) occurs when interstitial-type defects dominate the microstructure, and that deformation twinning tends to occur when the microstructure is relatively free of irradiationinduced defects.

Conclusions & knowledge gaps

We have reviewed the effect of irradiation on the deformation-induced martensitic phase transformation. Irradiation reduces the SFE through the introduction of a high density of defect clusters as well as microchemical segregation, leading to Shockley partial dissociation and thus activation of the $\gamma \rightarrow \alpha'$ martensitic transformation. Highly localized spatial modulations in SFE associated with irradiation-induced defects can also be sufficient to enable the nucleation, propagation, and

© Materials Research Society 2020 cambridge.org/JMR



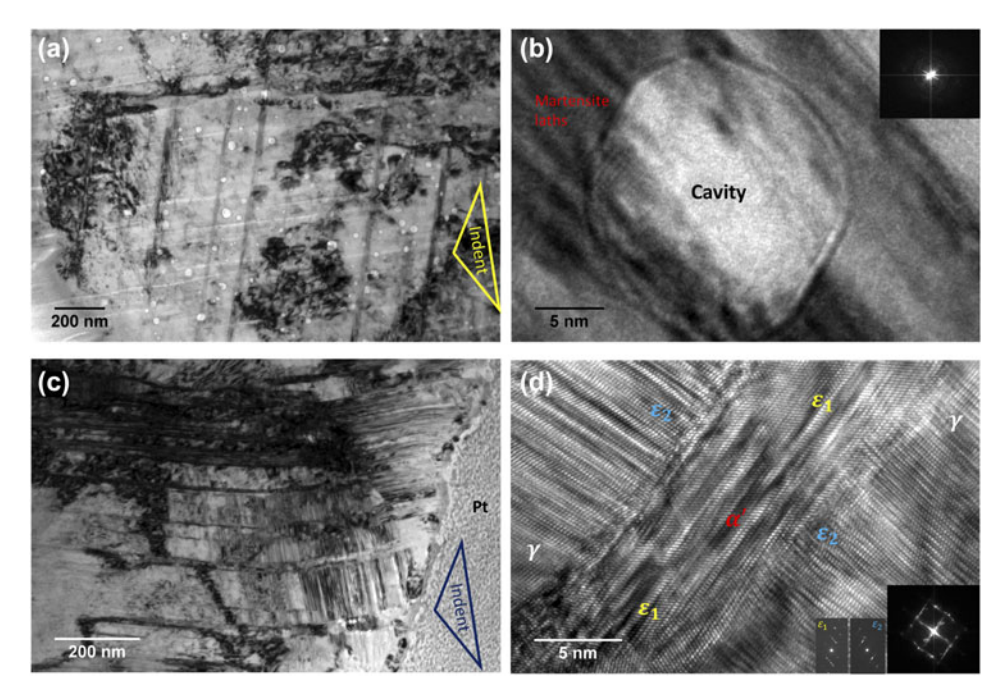


Figure 6: Post-nanoindent microstructure of (a) 23 dpa irradiated 304 SS with (b) HRTEM of martensite interacting with void; and (c) weld HAZ with (d) HRTEM image of formation of α' at intersection of two ϵ plates, adapted from Ref. 9. (color online)

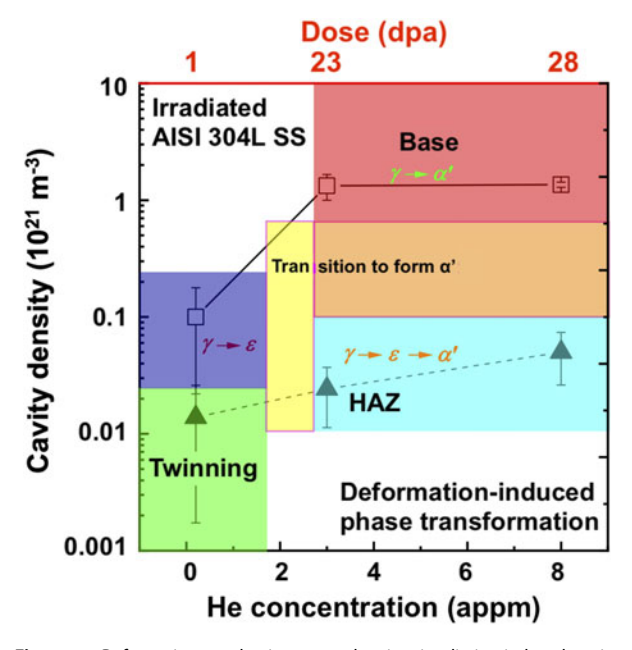


Figure 7: Deformation mechanism map showing irradiation-induced cavity density and He concentration influence the tendency for twinning, the $\gamma \to \epsilon \to \alpha'$ transformation, and the direct $\gamma \to \alpha'$ transformation, extrapolated from deformation studies on EBR-II irradiated AISI 304L SS from Mao et al. [9, 80, 83]. (color online)

termination of martensite needles through a nano-through microscopic volume of material. Irradiation-induced cavities are believed to play a central role in activating the martensitic transformation, either through contributing surface energy toward the total free energy of the material, and/or by hindering partial dislocation glide. The relative size and number density of cavities governs which stress-induced martensitic transform pathway, $\gamma \to \alpha'$ or $\gamma \to \epsilon \to \alpha'$, is active. That is, cavities can inhibit twinning—and thus encourage the martensitic transformation—if their number density is sufficiently high so as to enhance dislocation climb, or if their size is sufficiently large to enable partial dislocation recombination. A deformation mechanism map, with axes of irradiation-induced cavity morphology and He concentration, is generated based on reports in the archival literature on irradiated 304L SS, alluding to the relative roles of vacancy-type and interstitial-type irradiation defects on modulating the martensitic transformation pathway.

This article also highlights, however, that previous studies of irradiation effects on deformation-induced phase transformations are relatively inconclusive. There is a notable lack of systematic, controlled experiments, which has limited our understanding of the effect of irradiation fluence, temperature, or particle type, on deformation mechanisms. Moreover, there remains a knowledge gap on the role of individual irradiation defects on the deformation-induced martensitic transformation —such an understanding is partly hampered by the complexity of irradiated microstructures. That is, irradiated metals and alloys typically contain a confluence of a high number density of features, including dislocation loops, voids, bubbles, precipitates, and local composition gradients. It is difficult to isolate individual features—especially experimentally—to ascertain their role on deformation mechanisms. Numerous other factors are also known to generally influence deformation, including

grain orientation, Taylor and Schmid factors, grain boundaries, initial dislocation density (e.g., extent of cold work), and austenite stability [95]; these factors must also be considered in the context of irradiation. Additionally, this article has not distinguished voids from bubbles, and has instead treated both features under the more general term of "cavities." However, bubbles contain an internal gas pressure that can often exceed the yield strength of the material [30]; the role of this internal stress and its interaction with externally applied mechanical load has not yet been studied.

Acknowledgments

This work was supported by the U.S. Department of Energy, Office of Science, Basic Energy Sciences, Early Career Research Program, under award DE-SC0020150.

References

- Z. Jiao and G.S. Was: The role of irradiated microstructure in the localized deformation of austenitic stainless steels. *J. Nucl. Mater.* 407, 34–43 (2010).
- T.S. Byun, N. Hashimoto, K. Farrell, and E.H. Lee: Characteristics
 of microscopic strain localization in irradiated 316 stainless steels and
 pure vanadium. *J. Nucl. Mater.* 349, 251–264 (2006).
- M.D. McMurtrey, G.S. Was, B. Cui, I. Robertson, L. Smith, and D. Farkas: Strain localization at dislocation channel–grain boundary intersections in irradiated stainless steel. *Int. J. Plast.* 56, 219–231 (2014).
- **4. T.S. Byun**: On the stress dependence of partial dislocation separation and deformation microstructure in austenitic stainless steels. *Acta Mater.* **51**, 3063–3071 (2003).
- M.D. McMurtrey, B. Cui, I. Robertson, D. Farkas, and G.S. Was: Mechanism of dislocation channel-induced irradiation assisted stress corrosion crack initiation in austenitic stainless steel. *Curr. Opin. Solid State Mater. Sci.* 19, 305–314 (2015).
- A. Reichardt, A. Lupinacci, D. Frazer, N. Bailey, H. Vo,
 C. Howard, Z. Jiao, A.M. Minor, P. Chou, and P. Hosemann:
 Nanoindentation and in situ microcompression in different dose regimes of proton beam irradiated 304 SS. *J. Nucl. Mater.* 486, 323–331 (2017).
- E.H. Lee, T.S. Byun, J.D. Hunn, M.H. Yoo, K. Farrell, and L.K. Mansur: On the origin of deformation microstructures in austenitic stainless steel: Part I—microstructures. *Acta Mater.* 49, 3269–3276 (2001).
- M.N. Gussev, K.G. Field, and J.T. Busby: Strain-induced phase transformation at the surface of an AISI-304 stainless steel irradiated to 4.4 dpa and deformed to 0.8% strain. *J. Nucl. Mater.* 446, 187–192 (2014).
- K.S. Mao, C. Sun, Y. Huang, C-H. Shiau, F.A. Garner,
 P.D. Freyer, and J.P. Wharry: Grain orientation dependence of

- nanoindentation and deformation-induced martensitic phase transformation in neutron irradiated AISI 304L stainless steel. *Materialia* 5, 100208 (2019).
- 10. G.M. De Bellefon and J.C. Van Duysen: Tailoring plasticity of austenitic stainless steels for nuclear applications: Review of mechanisms controlling plasticity of austenitic steels below 400 °C. J. Nucl. Mater. 475, 168–191 (2016).
- N. Hashimoto and T.S. Byun: Deformation-induced martensite formation and dislocation channeling in neutron-irradiated 316 stainless steel. *J. Nucl. Mater.* 367–370, 960–965 (2007).
- 12. T.S. Byun, N. Hashimoto, and K. Farrell: Temperature dependence of strain hardening and plastic instability behaviors in austenitic stainless steels. *Acta Mater.* 52, 3889–3899 (2004).
- A.H. Cottrell and B.A. Bilby: LX. A mechanism for the growth of deformation twins in crystals. *Philos. Mag.* 42, 573–581 (1951).
- **14. J.A. Venables**: The martensite transformation in stainless steel. *Philos. Mag.* **7**, 35–44 (1961).
- J.A. Venables: Deformation twinning in face-centred cubic metals. Philos. Mag. 6, 379–396 (1961).
- N. Hashimoto, S.J. Zinkle, A.F. Rowcliffe, J.P. Robertson, and S. Jitsukawa: Deformation mechanisms in 316 stainless steel irradiated at 60 °C and 330 °C. J. Nucl. Mater. 283–287, 528–534 (2000).
- M. Chmielus, X.X. Zhang, C. Witherspoon, D.C. Dunand, and P. Müllner: Giant magnetic-field-induced strains in polycrystalline Ni–Mn–Ga foams. *Nat. Mater.* 8, 863–866 (2009).
- 18. W.Z. Han, J. Zhang, M.S. Ding, L. Lv, W.H. Wang, G.H. Wu, Z.W. Shan, and J. Li: Helium nanobubbles enhance superelasticity and retard shear localization in small-volume shape memory alloy. *Nano Lett.* 17, 3725–3730 (2017).
- 19. V.A. Levin, V.I. Levitas, K.M. Zingerman, and E.I. Freiman: Phase-field simulation of stress-induced martensitic phase transformations at large strains. *Int. J. Solid Struct.* 50, 2914–2928 (2013).
- 20. S. Martin, S. Wolf, U. Martin, L. Krüger, and D. Rafaja: Deformation mechanisms in austenitic TRIP/TWIP steel as a function of temperature. *Metall. Mater. Trans. A* 47, 49–58 (2016)
- 21. D.T. Pierce, J.A. Jiménez, J. Bentley, D. Raabe, and J.E. Wittig: The influence of stacking fault energy on the microstructural and strain-hardening evolution of Fe–Mn–Al–Si steels during tensile deformation. *Acta Mater.* 100, 178–190 (2015).
- 22. E.I. Galindo-Nava and P.E.J. Rivera-Díaz-del-Castillo: Understanding martensite and twin formation in austenitic steels: A model describing TRIP and TWIP effects. Acta Mater. 128, 120–134 (2017).
- K.H. Lo, C.H. Shek, and J.K.L. Lai: Recent developments in stainless steels. Mater. Sci. Eng. R Rep. 65, 39–104 (2009).
- **24. R.J. Wasilewski**: On the nature of the martensitic transformation. *Metall. Trans. A* **6**, 1405–1418 (1975).



10

11

12

13 14

15

16

17

18

19

20 21

23

24

25

26 27

28

29

30

31

32

33 34

35

36

37

38

39 40

41

42

43

44

45

46 47

48

49

50

51

52 53

54

55

56

57

58

59

60

AU4

- 25. J. Lu, L. Hultman, E. Holmström, K.H. Antonsson, M. Grehk, W. Li, L. Vitos, and A. Golpayegani: Stacking fault energies in austenitic stainless steels. Acta Mater. 111, 39-46 (2016).
- 26. R.G. Stringfellow, D.M. Parks, and G.B. Olson: A constitutive model for transformation plasticity accompanying strain-induced martensitic transformations in metastable austenitic steels. Acta Metall. Mater. 40, 1703-1716 (1992).
- 27. G.B. Olson and M. Cohen: Kinetics of strain-induced martensitic nucleation. Metall. Trans. A 6, 791-795 (1975).
- 28. W. Han, Q. Zhan, X. Yi, S. Ohnuki, Y. Liu, P. Liu, F. Wan, and D. Morrall: Deformation behavior of austenitic stainless steel at deep cryogenic temperatures. J. Nucl. Mater. 504, 29-32 (2018).
- 29. D. Guzonas, R. Novotny, S. Penttilä, A. Toivonen, and W. Zheng: Radiation effects and mechanical properties. In Materials and Water Chemistry for Supercritical Water-Cooled Reactors (Woodhead Publishing, 2018); pp. 45-78.
- 30. G.S. Was: Fundamentals of Radiation Materials Science: Metals and Alloys, 2nd ed. (Springer, New York, 2017).
- 31. K.C. Russell and R.W. Powell: Dislocation loop nucleation in irradiated metals. Acta Metall. 21, 187-193 (1973).
- 32. M. Hernández-Mayoral and M.J. Caturla: Microstructure evolution of irradiated structural materials in nuclear power plants. In Understanding and Mitigating Ageing in Nuclear Power Plants (Woodhead Publishing, 2010); pp. 189-235.
- 33. G.S. Was and P.L. Andresen: Radiation damage to structural alloys in nuclear power plants: Mechanisms and remediation. In Structural Alloys for Power Plants (Woodhead Publishing, 2014); pp. 355-420.
- 34. T.S. Byun, N. Hashimoto, and K. Farrell: Deformation mode map of irradiated 316 stainless steel in true stress-dose space. J. Nucl. Mater. 351, 303-315 (2006).
- 35. Y. Cui, G. Po, and N. Ghoniem: Does irradiation enhance or inhibit strain bursts at the submicron scale? Acta Mater. 132, 285-297 (2017).
- 36. J. Robach, I.M. Robertson, B.D. Wirth, and A. Arsenlis: In-situ transmission electron microscopy observations and molecular dynamics simulations of dislocation- defect interactions in ionirradiated copper. Philos. Mag. 83, 955-967 (2003).
- 37. G. Po and N. Ghoniem: Continuum modeling of plastic flow localization in irradiated fcc metals. J. Nucl. Mater. 442, S607-S611 (2013).
- 38. E.A. West, M.D. McMurtrey, Z. Jiao, and G.S. Was: Role of localized deformation in irradiation-assisted stress corrosion cracking initiation. Metall. Mater. Trans. A 43, 136-146 (2012).
- 39. T. Diaz De La Rubia, H.M. Zblb, T.A. Khralshl, B.D. Wirth, M. Victoria, and M.J. Caturia: Multiscale modelling of plastic flow localization in irradiated materials. Nature 406, 871-874 (2000).
- 40. J. Kacher, G.S. Liu, and I.M. Robertson: In situ and tomographic observations of defect free channel formation in ion irradiated stainless steels. Micron 43, 1099-1107 (2012).
- 41. M.N. Gussev, K.G. Field, and J.T. Busby: Deformation localization and dislocation channel dynamics in neutron-

- irradiated austenitic stainless steels. J. Nucl. Mater. 460, 139-152
- 42. C.R.F. Azevedo: A review on neutron-irradiation-induced hardening of metallic components. Eng. Fail. Anal. 18, 1921-1942
- 43. G.S. Was, D. Farkas, and I.M. Robertson: Micromechanics of dislocation channeling in intergranular stress corrosion crack nucleation. Curr. Opin. Solid State Mater. Sci. 16, 134-142 (2012).
- 44. T.S. Byun and N. Hashimoto: Strain localization in irradiated materials. Nucl. Eng. Technol. 38, 619-638 (2006).
- 45. T.S. Byun, K. Farrell, and M. Li: Deformation in metals after lowtemperature irradiation: Part I-Mapping macroscopic deformation modes on true stress-dose plane. Acta Mater. 56, 1044-1055 (2008).
- 46. E.H. Lee, T.S. Byun, J.D. Hunn, M.H. Yoo, K. Farrell, and L.K. Mansur: On the origin of deformation microstructures in austenitic stainless steel: Part II-Mechanisms. Acta Mater. 49, 3277-3287 (2001).
- 47. E.H. Lee, T.S. Byun, J.D. Hunn, K. Farrell, and L.K. Mansur: Origin of hardening and deformation mechanisms in irradiated 316 LN austenitic stainless steel. J. Nucl. Mater. 296, 183-191 (2001).
- 48. T.S. Byun, E.H. Lee, and J.D. Hunn: Plastic deformation in 316LN stainless steel-Characterization of deformation microstructures. J. Nucl. Mater. 321, 29-39 (2003).
- 49. T.S. Byun and K. Farrell: Plastic instability in polycrystalline metals after low temperature irradiation. Acta Mater. 52, 1597-1608 (2004).
- 50. K. Farrell, T.S. Byun, and N. Hashimoto: Deformation mode maps for tensile deformation of neutron-irradiated structural alloys. J. Nucl. Mater. 335, 471-486 (2004).
- 51. H.N. Han, C.G. Lee, C-S. Oh, T-H. Lee, and S-J. Kim: A model for deformation behavior and mechanically induced martensitic transformation of metastable austenitic steel. Acta Mater. 52, 5203-5214 (2004).
- 52. F. Roters, P. Eisenlohr, L. Hantcherli, D.D. Tjahjanto, T.R. Bieler, and D. Raabe: Overview of constitutive laws, kinematics, homogenization and multiscale methods in crystal plasticity finite-element modeling: Theory, experiments, applications. Acta Mater. 58, 1152-1211 (2010).
- 53. X-S. Yang, S. Sun, X-L. Wu, E. Ma, and T-Y. Zhang: Dissecting the mechanism of martensitic transformation via atomic-scale observations. Sci. Rep. 4, 6141 (2015).
- 54. Y.F. Shen, X.X. Li, X. Sun, Y.D. Wang, and L. Zuo: Twinning and martensite in a 304 austenitic stainless steel. Mater. Sci. Eng., A 552, 514-522 (2012).
- 55. C.X. Huang, G. Yang, Y.L. Gao, S.D. Wu, and S.X. Li: Investigation on the nucleation mechanism of deformationinduced martensite in an austenitic stainless steel under severe plastic deformation. J. Mater. Res. 22, 724-729 (2007).

58 59

60

AU5

2

3



- 56. M.N. Gusev, O.P. Maksimkin, and F.A. Garner: Peculiarities of plastic flow involving "deformation waves" observed during lowtemperature tensile tests of highly irradiated 12Cr18Ni10Ti and 08Cr16Ni11Mo3 steels. J. Nucl. Mater. 403, 121-125 (2010).
- 57. K.G. Field, M.N. Gussev, and J.T. Busby: Microstructural characterization of deformation localization at small strains in a neutronirradiated 304 stainless steel. J. Nucl. Mater. 452, 500-508 (2014).
- 58. M-S. Ding, J-P. Du, L. Wan, S. Ogata, L. Tian, E. Ma, W-Z. Han, J. Li, and Z-W. Shan: Radiation-induced helium nanobubbles enhance ductility in submicron-sized single-crystalline copper. Nano Lett. 16, 4118-4124 (2016).
- 59. M.N. Gussev, J.T. Busby, and F.A. Garner: Phase instability and martensitic transformation as a potential degradation mode of nuclear plant internal components. In International Conference on Environmental Degradation of Materials in Nuclear Power Systems -Water Reactors (2015); pp. 1-10.
- 60. A. Renault-Laborne, J. Hure, J. Malaplate, P. Gavoille, F. Sefta, and B. Tanguy: Tensile properties and deformation microstructure of highly neutron-irradiated 316 stainless steels at low and fast strain rate. J. Nucl. Mater. 508, 488-504 (2018).
- 61. J.I. Cole and S.M. Bruemmer: Post-irradiation deformation characteristics of heavy-ion irradiated 304L SS. J. Nucl. Mater. 225,
- 62. D. Alontseva, O. Maksimkin, A. Russakova, and S. Suslov: $\gamma \rightarrow \alpha$ martensitic transformation in the reactor steels under irradiation and deformation. Mater. Sci. 20, 15-20 (2014).
- 63. X. Li and A. Almazouzi: Deformation and microstructure of neutron irradiated stainless steels with different stacking fault energy. J. Nucl. Mater. 385, 329-333 (2009).
- 64. S. Curtze, V.T. Kuokkala, A. Oikari, J. Talonen, and H. Hänninen: Thermodynamic modeling of the stacking fault energy of austenitic steels. Acta Mater. 59, 1068-1076 (2011).
- 65. P.J. Doyle, K.M. Benensky, and S.J. Zinkle: Modeling of dislocation channel width evolution in irradiated metals. J. Nucl. Mater. 499, 47-64 (2018).
- 66. R.M. Latanision and A.W. Ruff: The temperature dependence of stacking fault energy in Fe-Cr-Ni alloys. Metall. Trans. 2, 505-509 (1971).
- 67. T. Hickel, S. Sandlöbes, R.K.W. Marceau, A. Dick, I. Bleskov, J. Neugebauer, and D. Raabe: Impact of nanodiffusion on the stacking fault energy in high-strength steels. Acta Mater. 75, 147-
- 68. R.E. Stoltz and J.B. Vander Sande: The effect of nitrogen on stacking fault energy of Fe-Ni-Cr-Mn steels. Metall. Trans. A 11, 1033-1037 (1980).
- 69. I.A. Yakubtsov, A. Ariapour, and D.D. Perovic: Effect of nitrogen on stacking fault energy of f.c.c. iron-based alloys. Acta Mater. 47, 1271-1279 (1999).
- 70. L. Vitos, J.O. Nilsson, and B. Johansson: Alloving effects on the stacking fault energy in austenitic stainless steels from firstprinciples theory. Acta Mater. 54, 3821-3826 (2006).

- 71. L. Remy: Temperature variation of the intrinsic stacking fault energy of a high manganese austenitic steel. Acta Metall. 25, 173-179 (1977).
- 72. E. Asadi, M.A. Zaeem, A. Moitra, and M.A. Tschopp: Effect of vacancy defects on generalized stacking fault energy of fcc metals. J. Phys. Condens. Matter 26 (2014).
- 73. J-H. Jun and C-S. Choi: Variation of stacking fault energy with austenite grain size and its effect on the MS temperature of $\gamma \to \epsilon$ martensitic transformation in Fe-Mn alloy. Mater. Sci. Eng., A 257, 353-356 (1998).
- 74. J-Y. Choi and W. Jin: Strain induced martensite formation and its effect on strain hardening behavior in the cold drawn 304 austenitic stainless steels. Scr. Mater. 36, 99-104 (1997).
- 75. J.P. Wharry, K.H. Yano, and P.V. Patki: Intrinsic-extrinsic size effect relationship for micromechanical tests. Scr. Mater. 162, 63-67 (2019).
- 76. G.S. Was, J.P. Wharry, B. Frisbie, B.D. Wirth, D. Morgan, J.D. Tucker, and T.R. Allen: Assessment of radiation-induced segregation mechanisms in austenitic and ferritic-martensitic alloys. J. Nucl. Mater. 411, 41-50 (2011).
- 77. S. Zhao, Y. Osetsky, G.M. Stocks, and Y. Zhang: Localenvironment dependence of stacking fault energies in concentrated solid-solution alloys. npj Comput. Mater. 5, 1-7 (2019).
- 78. S.L. Altmann, C.A. Coulson, and W. Hume-Rothery: On the relation between bond hybrids and the metallic structures. Proc. Roy. Soc. Lond. Math. Phys. Sci. 240, 145-159 (1957).
- 79. I.R. Harris, I.L. Dillamore, R.E. Smallman, and B.E.P. Beeston: The influence of d-band structure on stacking-fault energy. Philos. Mag. 14, 325-333 (1966).
- 80. K.S. Mao, C. Sun, C-H. Shiau, K.H. Yano, P.D. Freyer, A.A. El-Azab, F.A. Garner, A. French, L. Shao, and J.P. Wharry: Role of cavities on deformation-induced martensitic transformation pathways in a laser-welded, neutron irradiated austenitic stainless steel. Scr. Mater. 178, 1-6 (2020).
- 81. M.S. Ding, L. Tian, W.Z. Han, J. Li, E. Ma, and Z.W. Shan: Nanobubble fragmentation and bubble-free-channel shear localization in helium-irradiated submicron-sized copper. Phys. Rev. Lett. 117, 215501 (2016).
- 82. M.N. Gussev, J.T. Busby, and F.A. Garner: Phase instability and martensitic transformation as a potential degradation mode of nuclear plant internal components. In International Conference on Environmental Degradation of Materials in Nuclear Power Systems-Water Reactors (Ottawa, Ontario, Canada, 2015); pp. 1-10.
- 83. K.S. Mao, C. Sun, X. Liu, H.J. Qu, A.J. French, P.D. Freyer, F.A. Garner, L. Shao, and J.P. Wharry: Effect of laser welding on deformation mechanisms in irradiated austenitic stainless steel. J. Nucl. Mater. 528, 151878 (2020).
- 84. K. Mao, H. Wang, Y. Wu, V. Tomar, and J.P. Wharry: Microstructure-property relationship for AISI 304/308L stainless steel laser weldment. Mater. Sci. Eng., A 721, 234-243 (2018).

cambridge.org/JMR



- 85. K.S. Mao, Y. Wu, C. Sun, E. Perez, and J.P. Wharry: Laser weld-induced formation of amorphous Mn-Si precipitate in 304 stainless steel. *Materialia* 3, 174-177 (2018).
- **86. M. Ortiz and A. Molinari**: Effect of strain hardening and rate sensitivity on the dynamic growth of a void in a plastic material. *J. Appl. Mech.* **59**, 48 (1992).
- 87. Y.N. Osetsky and D.J. Bacon: Atomic-scale mechanisms of void hardening in bcc and fcc metals. *Philos. Mag.* **90**, 945–961 (2010).
- 88. T-H. Ahn, C-S. Oh, D.H. Kim, K.H. Oh, H. Bei, E.P. George, and H.N. Han: Investigation of strain-induced martensitic transformation in metastable austenite using nanoindentation. Scr. Mater. 63, 540–543 (2010).
- **89. A. Bogers and W. Burgers**: Partial dislocations on the {110} planes in the B.C.C. lattice and the transition of the F.C.C. into the B.C.C. lattice. *Acta Metall.* **12**, 255–261 (1964).

- **90. G.B. Olson and M. Cohen**: A mechanism for the strain-induced nucleation of martensitic transformations. *J. Less Common Met.* **28**, 107–118 (1972).
- **91.** J. Christian and J.W. Christian: Twinning and martensitic transformation. *J. Phys. Collo-Ques.* **35**, C7 (1974).
- **92.** W.Z. Han, M.S. Ding, R.L. Narayan, and Z-W. Shan: In situ study of deformation twinning and detwinning in helium irradiated small-volume copper. *Adv. Eng. Mater.* **19**, 1700357 (2017).
- 93. K. Doihara, T. Okita, M. Itakura, M. Aichi, and K. Suzuki: Atomic simulations to evaluate effects of stacking fault energy on interactions between edge dislocation and spherical void in facecentred cubic metals. *Philos. Mag.* 98, 2061–2076 (2018).
- 94. D.J. Edwards, E.P. Simonen, and S.M. Bruemmer: Evolution of fine-scale defects in stainless steels neutron-irradiated at 275 °C. J. Nucl. Mater. 317, 13–31 (2003).
- **95. M.A. Meyers and K.K. Chawla**: *Mechanical Behavior of Materials*, 2nd ed. (Cambridge University Press, 2008).



AUTHOR QUERY - jmr.2020.80

- 1 Please provide the department (if any) for all affiliations.
- 2 Please provide the expansion for TEM and HRTEM.
- 3 Details given in references '11' and '65' were same. Hence, reference '65' has been deleted and the references have been renumbered accordingly.
- 4 Please provide the editors name and publisher location for references '29, 32, and 33'.
- [5] Please provide the editors name, publisher name, and location for reference '59'.
- [6] Please provide the editors name and publisher name for reference '82'.
- 7 Please provide the publisher location for reference '95'.

EDITOR QUERY - jmr.2020.80

There are no editor queries for this article.